ORGANISMAL BIOLOGY

Feeding diverse prey as an excellent strategy of mixotrophic dinoflagellates for global dominance

Hae Jin Jeong[1]*, Hee Chang Kang[1]*, An Suk Lim[2], Se Hyeon Jang[1], Kitack Lee[3], Sung Yeon Lee[1], Jin Hee Ok[1], Ji Hyun You[1], Ji Hye Kim[1], Kyung Ha Lee[1], Sang Ah Park[1], Se Hee Eom[1], Yeong Du Yoo[4], Kwang Young Kim[5]

Microalgae fuel food webs and biogeochemical cycles of key elements in the ocean. What determines microalgal dominance in the ocean is a long-standing question. Red tide distribution data (spanning 1990 to 2019) show that mixotrophic dinoflagellates, capable of photosynthesis and predation together, were responsible for ~40% of the species forming red tides globally. Counterintuitively, the species with low or moderate growth rates but diverse prey including diatoms caused red tides globally. The ability of these dinoflagellates to trade off growth for prey diversity is another genetic factor critical to formation of red tides across diverse ocean conditions. This finding has profound implications for explaining the global dominance of particular microalgae, their key eco-evolutionary strategy, and prediction of harmful red tide outbreaks.

INTRODUCTION

Microalgae play critical roles in atmospheric oxygen production, food webs, and element cycles (*1*–*4*). They have dominated in past and present oceans (*5*–*7*). In the Cenozoic ocean, diatoms dominated, whereas dinoflagellates and coccolithophorids declined (*8*). However, a particular group of mixotrophic dinoflagellates dominates in "this diatom-dominated contemporary ocean" (*9*, *10*). Usually, only one or a few species dominate the microalgal assemblages through severe competition, and this dominance is visible as a red tide, which is a discoloration at the sea surface (*9*). Red tides dominated by mixotrophic dinoflagellates often cause human illness, large-scale mortality of diverse organisms, and great losses to the aquaculture and tourist industries (*11*, *12*). Thus, identifying a particular species or group of mixotrophic dinoflagellates predominating in the global ocean and understanding their eco-physiological characteristics and eco-evolutionary strategies are critical and challenging tasks for scientists.

To reveal their strategies for predominating in the global ocean, mixotrophic dinoflagellates should be categorized to several subgroups on the basis of their mixotrophic abilities and global dominance. Previous studies divided mixotrophic dinoflagellates into one or a few categories at the community level, but not many categories at the species level (*13*–*15*). Thus, the eco-evolutionary strategies of a particular species or group of mixotrophic dinoflagellates to dominate in the global ocean have been poorly explored to date.

RESULTS AND DISCUSSION

Red tide species

We explored red tide distributions, presence or absence of target genes related to photosynthesis of dinoflagellates, and mixotrophic ability of the target mixotrophic dinoflagellates (Supplementary Materials). In the world ocean in 1990–2019, of 37,911 microalgal and cyanobacterial species, only 365 species have been reported to cause red tides (table S1). The portion of dinoflagellates was 36% of total red tide species, although that was only 9% of total microalgal species (Fig. 1, A and B, and table S1). The numbers of species causing red tides in the waters of ≥10 countries (hereafter the species causing red tides globally) were 17 diatoms (50%), 15 dinoflagellates (44%), 1 haptophyte (3%), and 1 cyanobacterium species (3%) (Fig. 1C and figs. S1 and S2). Of the 15 dinoflagellates, 13 species were mixotrophic, 1 kleptoplastidic, and 1 heterotrophic (Fig. 1D). Mixotrophic dinoflagellates have their own chloroplasts, but kleptoplastidic dinoflagellates require chloroplasts of ingested prey (*16*–*19*). Although these 13 mixotrophic dinoflagellates caused red tides globally, many other mixotrophic dinoflagellates caused local or no red tides (Fig. 1, E and F, and tables S2 and S3). Thus, the mixotrophic dinoflagellates causing red tides globally may have some advantageous tools over those causing local or no red tides.

Presence of photosynthesis genes

We investigated the presence of the 22 target genes related to three major parts of photosynthesis of 17 dinoflagellates having different trophic modes (Fig. 2 and tables S4 to S10). There was no difference among the mixotrophic dinoflagellates and also between mixotrophic and autotrophic dinoflagellates. However, there were big differences between mixotrophic and heterotrophic dinoflagellates (Fig. 2). In contrast, there was a higher similarity in the presence of the genes between kleptoplastidic and heterotrophic dinoflagellates than between kleptoplastidic and mixotrophic dinoflagellates, indicating that the trophic nature of the kleptoplastidic dinoflagellates may be closer to that of heterotrophic dinoflagellates (Fig. 2). The signal of the presence of some genes related to the photosystems of the kleptoplastidic dinoflagellates *Gymnodinium smaydae* and *Pfiesteria piscicida* shown in the transcriptome datasets came from *Heterocapsa* spp. and diatoms (fig. S3), and that of *Dinophysis acuminata* from haptophytes (fig. S4).

Indices for the mixotrophic ability

We proposed two indices for the mixotrophic ability of the target mixotrophic dinoflagellates and *G. smaydae*—predation contribution

[1]School of Earth and Environmental Sciences, Seoul National University, Seoul 08826, Korea. [2]Division of Life Science and Plant Molecular Biology and Biotechnology Research Center, Gyeongsang National University, Jinju 52828, Korea. [3]Division of Environmental Science and Engineering, Pohang University of Science and Technology, Pohang 37673, Korea. [4]Faculty of Marine Applied Biosciences, Kunsan National University, Gunsan 54150, Korea. [5]Department of Oceanography, Chonnam National University, Gwangju, Korea.
*Corresponding author. Email: hjjeong@snu.ac.kr (H.J.J.); gmlckd5457@snu.ac.kr (H.C.K.)

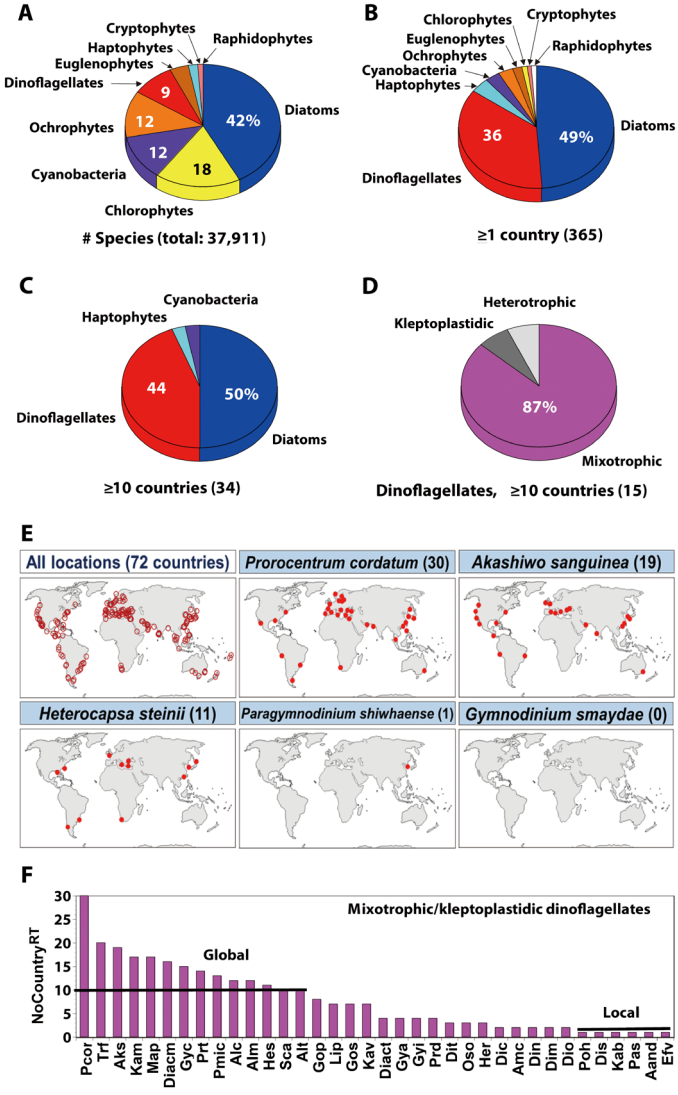

Fig. 1. Red tide dinoflagellates. (**A**) Ratio (%) of the species number of each group relative to that of the formally described microalgae (table S1). Ratio (%) of the species number of each group relative to that of the microalgae that caused red tides in the waters of ≥1 country (**B**) and ≥10 countries (**C**) during 1990–2019. (**D**) Ratio (%) of mixotrophic, kleptoplastidic, and heterotrophic dinoflagellates among the dinoflagellates causing red tides in the waters of ≥10 countries (global species). (**E**) The countries where at least one red tide of dinoflagellates occurred during 1990–2019, and the countries where representative mixotrophic/kleptoplastidic dinoflagellates caused global, local, or no red tides. (**F**) The number of the countries in which red tides of the mixotrophic/kleptoplastidic dinoflagellates occurred during 1990–2019 (NoCountry^{RT}). The abbreviation of each mixotrophic dinoflagellate is listed in table S2.

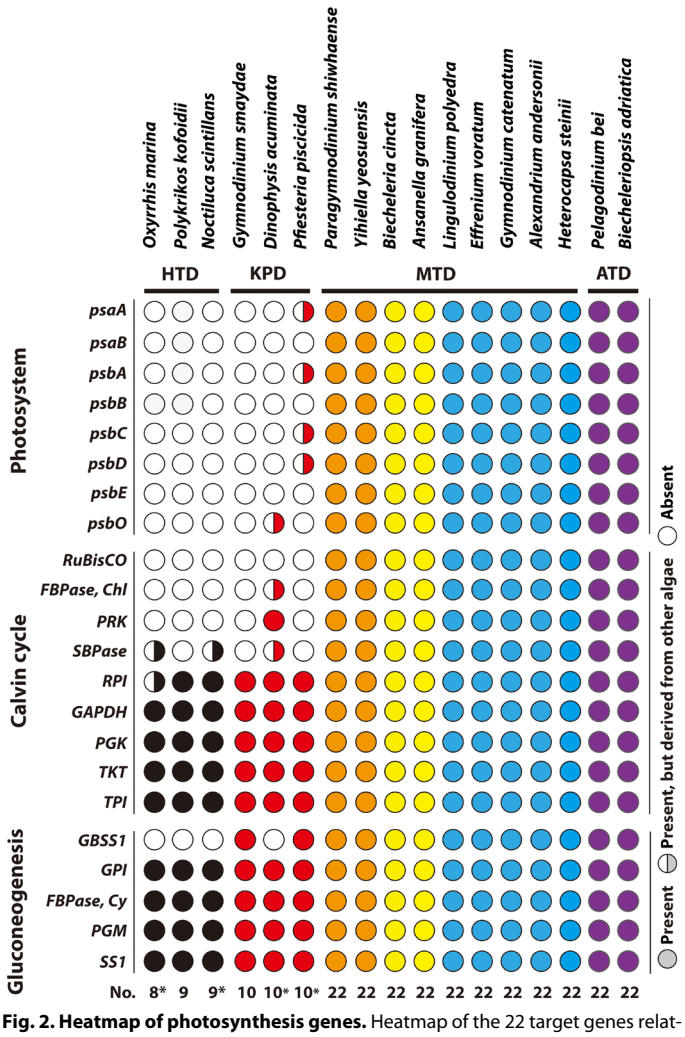

Fig. 2. Heatmap of photosynthesis genes. Heatmap of the 22 target genes related to photosystems, the Calvin cycle, and gluconeogenesis of 17 representing dinoflagellates including heterotrophic (HTD), kleptoplastidic (KPD), mixotrophic (MTD), and autotrophic (ATD) species (tables S4 to S10). The number of the identified genes are provided, but the horizontal gene transfer candidates have not been included (instead, marked as asterisks). The identified transcript ID and presence of the genes with abbreviation are listed in table S4.

to total growth rate (PredC^{TGR}) and the ratio of the number of edible prey taxa to that of total tested prey taxa (RET^{PREY}). The PredC^{TGR} of 20 target mixotrophic dinoflagellates and *G. smaydae* feeding on the optimal prey species under varying prey concentration, light, or temperature conditions showed a huge variation, ranging from 4 to 100% (Fig. 3, A to E, figs. S5 to S7, and table S11). Using this huge variation, we categorized these mixotrophic dinoflagellates into three subgroups (Fig. 3E); the mixotrophic dinoflagellate group having PredC^{TGR} of >60% (heterotrophy-dominant mixotrophic dinoflagellate) included *Paragymnodinium shiwhaense* and four others; those with PredC^{TGR} of >40 to 60% (neutral mixotrophic dinoflagellate) included *Takayama helix*; and those with PredC^{TGR} of 1 to 40% (autotrophy-dominant mixotrophic dinoflagellate) included *Margalefidinium polykrikoides* and 13 other species. Among the heterotrophy-dominant mixotrophic dinoflagellates, the mixotrophic dinoflagellates having PredC^{TGR} of >90% and at least one PredC^{TGR} value under diverse conditions reaching 100% were allocated to be the obligate mixotrophic dinoflagellates that included *P. shiwhaense* and *Yihiella yeosuensis*.

The RET^{PREY} of the 20 target mixotrophic dinoflagellates and *G. smaydae* also showed a huge variation, ranging from 6 to 100% (Fig. 3F). The RET^{PREY} of all heterotrophy-dominant mixotrophic dinoflagellates did not exceed 50%, whereas those of all autotrophy-dominant mixotrophic dinoflagellates except for *Effrenium voratum*, *Alexandrium andersonii*, and *Takayama tasmanica* exceeded 50%.

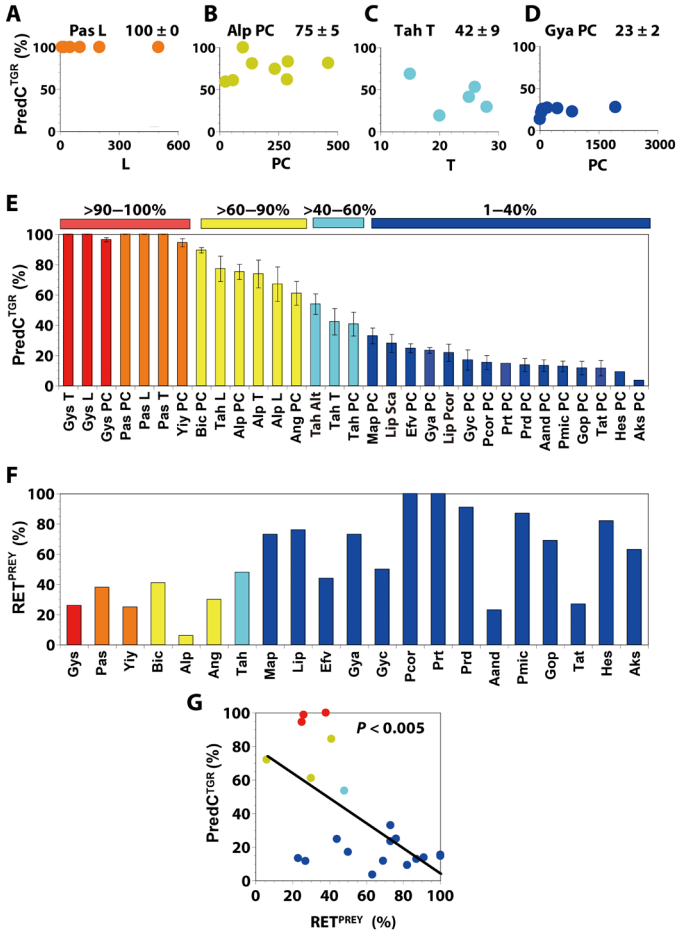

Fig. 3. Indices for the mixotrophic ability. (**A** to **D**) Predation contribution to total growth rate (PredC^{TGR}, %) of four representative mixotrophic dinoflagellates on the optimal prey as a function of prey concentration (PC; cells ml^{-1}), light intensity (L; μE m^{-2} s^{-1}), or temperature (T; °C). The numbers represent mean ± SE. Pas, *Paragymnodinium shiwhaense*; Alp, *Alexandrium pohangense*; Tah, *Takayama helix*; Gya, *Gymnodinium aureolum*. (**E**) PredC^{TGR} of each mixotrophic/kleptoplastidic dinoflagellate as a function of PC, L, or T. These mixotrophic/kleptoplastidic dinoflagellates are listed in table S11. (**F**) The ratio of the number of edible prey taxa to that of total tested prey taxa of each mixotrophic/kleptoplastidic dinoflagellate (RET^{PREY}, %). (**G**) PredC^{TGR} as a function of RET^{PREY} of the mixotrophic/kleptoplastidic dinoflagellate. The equation of the linear regression was as follows: (PredC^{TGR}) = −0.766 (RET^{PREY}) + 82.8, r^2 = 0.369.

The PredC^{TGR} of the target mixotrophic dinoflagellates and *G. smaydae* was inversely correlated with RET^{PREY} (Fig. 3G). Thus, PredC^{TGR} of the target mixotrophic dinoflagellates and *G. smaydae* was possibly traded off with RET^{PREY} in dinoflagellate evolution. To dominate, each mixotrophic dinoflagellate might have evolved to one of the two mixotrophic abilities. The negative correlation between PredC^{TGR} and RET^{PREY} can be explained as follows: Generally, animal predators that feed on one or a few preferred prey species (i.e., specialists) have higher foraging or feeding efficiencies than those that feed on diverse prey species (i.e., generalists) (*20*–*22*). Thus, mixotrophic dinoflagellates that feed on one or a few prey species (i.e., having low RET^{PREY}) will possibly have higher feeding efficiencies and, in turn, maximum growth rates than those of mixotrophic dinoflagellates that feed on diverse prey (i.e., having high RET^{PREY}). Higher maximum growth rates of mixotrophic dinoflagellates with low RET^{PREY} than those of mixotrophic dinoflagellates with high RET^{PREY} are responsible for higher PredC^{TGR} because the autotrophic growth rates of mixotrophic dinoflagellates with low RET^{PREY} were similar to or lower than those of the mixotrophic dinoflagellates with high RET^{PREY}.

Number of countries in which red tides of each species occur

The number of countries in which red tides of each species (NoCountry^{RT}) of all the target autotrophy-dominant mixotrophic dinoflagellates, except for *E. voratum*, *Gymnodinium aureolum*, *A. andersonii*, and *T. tasmanica*, occurred were >5. The NoCountry^{RT} of all target neutral and heterotrophy-dominant mixotrophic dinoflagellates were 0 or 1 (Fig. 4A). The NoCountry^{RT} of the target mixotrophic dinoflagellates was linearly correlated with their RET^{PREY} (Fig. 4B), but inversely correlated with the PredC^{TGR} (Fig. 4C). Moreover, the target mixotrophic dinoflagellates causing red tides globally had RET^{PREY} of >50% but PredC^{TGR} of <40%. Therefore, for the mixotrophic dinoflagellates to form red tides globally, having a mixotrophic ability to feed on diverse prey is more critical than relying on predation for growth. The NoCountry^{RT} of the target mixotrophic dinoflagellates was not significantly correlated with maximum growth rate (Fig. 4D); however, the target mixotrophic dinoflagellates that have low or moderate maximum growth rates of 0.5 to 0.9 day^{-1} (0.7 to 1.3 divisions per day) tended to lead to global occurrence of red tides, whereas those having maximum growth rates of >1.0 day^{-1} (>1.4 divisions per day) tended to lead one or no red tides. Thus, counterintuitively, the species having low or moderate growth rates, low predation contribution to total growth rate, but diverse prey caused red tides globally. Furthermore, the global red tide–forming mixotrophic dinoflagellates are able to feed on *Skeletonema costatum*, which is most commonly found diatom species (fig. S2), whereas the non–red tide–forming mixotrophic dinoflagellate species did not feed on this diatom (Fig. 4E). Among the autotrophy-dominant mixotrophic dinoflagellates, *E. voratum*, *G. aureolum*, *A. andersonii*, and *T. tasmanica* that did not feed on *S. costatum* caused few or no red tides (Fig. 4, A and E). Thus, having a mixotrophic ability of feeding on common diatoms is an eco-evolutionary strategy of mixotrophic dinoflagellates for dominance.

The kleptoplastidic dinoflagellate *G. smaydae* and obligate mixotrophic dinoflagellate *Y. yeosuensis* did not cause red tides, although they had the highest and third highest maximum growth rates (1.3 to 2.2 day^{-1}, two to three divisions per day) among the mixotrophic/kleptoplastidic dinoflagellates (Fig. 4A and fig. S8). Our intensive field studies confirmed this (*23*, *24*). They can grow almost only when feeding on prey. Their RET^{PREY} was considerably low (Fig. 3F); thus, a low chance of encountering edible prey prevents them from surviving unless edible prey is abundant. Their ability of growing as fast as some diatoms may not be a strategy for forming red tides.

Using the results of this study, we provided an insight into the eco-evolutionary strategies of the autotrophy-dominant mixotrophic dinoflagellates for dominating globally as follows: Autotrophy-dominant mixotrophic dinoflagellates trading off growth and predation contribution with prey diversity can survive by feeding on any of the many edible prey species under unfavorable photosynthesis conditions. However, diatoms that once grew fast and dominated nutrient-rich conditions would die under these unfavorable conditions. When the conditions for photosynthesis turn to be favorable, autotrophy-dominant mixotrophic dinoflagellates that survived can grow slowly or moderately but form red tides without competition

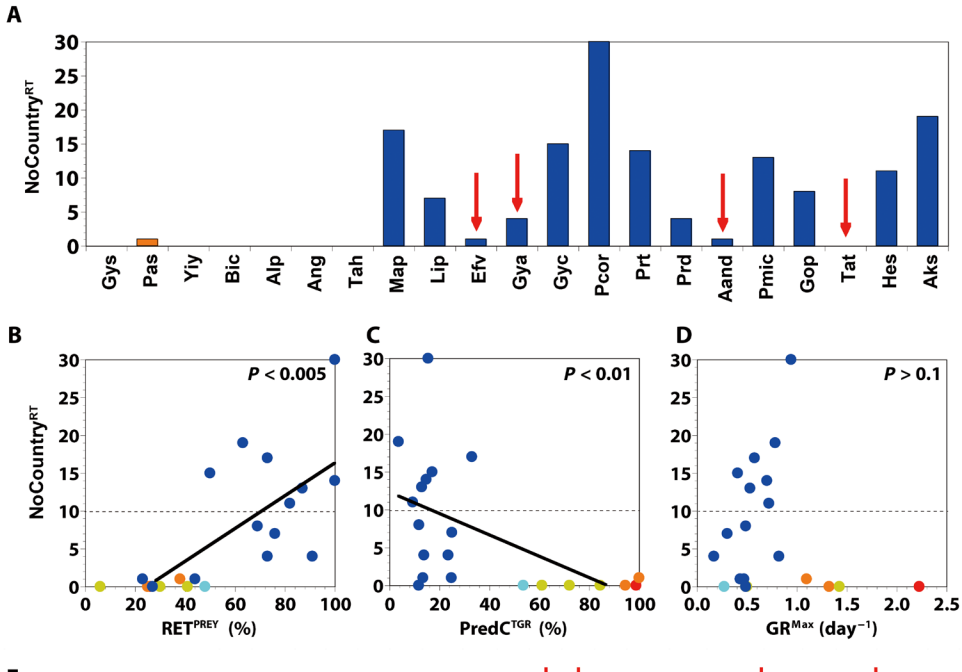

E

Predator	Gys	Pas	Yiy	Bic	Alp	Ang	Tah	Map	Lip	Efv	Gya	Gyc	Pcor	Prt	Prd	Aand	Pmic	Gop	Tat	Hes	Aks
Prey/feeding mechanism	PE	PE	EG	PE	EG	EG	SUCK	EG	EG	PE	EG	EG	EG	EG	EG	EG	EG	EG	SUCK	EG	EG
Skeletonema costatum (DIA)	X	X	X	X	X	X	X	O	O	X	X	O	O	O	O	X	O	O	X	O	O
Teleaulax amphioxeia (CRYP)	X	O	O	O	X	X	X	O	O	O	O	O	O	O	O	O	O	O	X	O	O
Isochrysis galbana (HAPT)	O	O	X	O	X	X	X	O	O	O	O	O	O	O	O	X	O	O	X	O	O
Heterosigma akashiwo (RAPH)	X	O	X	O	X	X	X	O	O	O	O	O	O	O	O	X	O	O	X	O	O
Amphidinium carterae (DINO)	X	O	X	O	X	X	X	O	O	O	O	O	O	O	O	X	O	O	X	O	O
Other dinoflagellate prey	4, O	2, O	X	2, O	1, O	X	16, O	1, O	7, O	2, O	2, O	2, O	1, O	2, O	2, O	1, O	5, O	4, O	9, O	2, O	6, O
RET^{PREY} (%)	26	38	25	41	6	33	48	73	76	44	73	50	100	100	91	23	87	69	27	82	68
$PredC^{TGR}$ (%)	99	100	95	84	72	61	54	33	25	25	24	17	15	15	14	13	13	12	12	9	4
$NoCountry^{RT}$	0	1	0	0	0	0	0	17	7	1	4	15	30	14	4	1	13	8	0	11	19

Fig. 4. Red tide distribution and feeding occurrence. (**A**) The number of the countries in which each target mixotrophic/kleptoplastidic dinoflagellate caused red tides during 1990–2019 ($NoCountry^{RT}$). $NoCountry^{RT}$ as a function of the ratio of the number of edible prey taxa to that of total tested prey taxa of each mixotrophic/kleptoplastidic dinoflagellate (RET^{PREY}) (**B**), and predation contribution to total growth rate ($PredC^{TGR}$) (**C**), and the maximum growth rate (GR^{Max}) (**D**). The equation of the linear regression was as follows: (B) $(NoCountry^{RT}) = 0.218\ (RET^{PREY}) - 5.17$, $r^2 = 0.561$; (C) $(NoCountry^{RT}) = -0.138\ (PredC^{TGR}) + 12$, $r^2 = 0.331$. (**E**) The feeding occurrence of the target mixotrophic/kleptoplastidic dinoflagellate on the common prey items (table S11). DIA, diatom; CRYP, cryptophyte; HAPT, haptophyte; RAPH, raphidophyte; DINO, dinophyte. Feeding mechanism: peduncle (PE), engulfment (EG), and sucking (SUCK). O with blue box indicates occurrence of feeding, whereas X with pink box indicates no occurrence of feeding. In dinoflagellate prey, the number in front of O indicates the number of O's. Pink boxes indicate RET^{PREY} of <50%, $PredC^{TGR}$ of <50%, or $NoCountry^{RT}$ of <5, whereas blue boxes indicate RET^{PREY} of ≥50%, $PredC^{TGR}$ of ≥50%, or $NoCountry^{RT}$ of ≥5. Red arrows in (A) and (E) indicate the mixotrophic dinoflagellates with $PredC^{TGR}$ of <50% and $NoCountry^{RT}$ of <5. These dinoflagellates did not feed on *Skeletonema costatum*.

with heterotrophy-dominant mixotrophic dinoflagellates or diatoms that have already vanished during the period of nutrient and edible prey limitation. The autotrophy-dominant mixotrophic dinoflagellates capable of efficient photosynthesis but marginal predation activity on diverse prey have a greater advantage in forming red tides across diverse ocean conditions. Therefore, for mixotrophic dinoflagellates' global red tide formation, survival is more important than fast growth, and thus, trading off predation contribution for diverse prey is an excellent strategy. Such assets must have been acquired through evolution, and the trade-off is another critical genetic aspect of forming red tides across diverse ocean conditions. Unveiling the strategy in contemporary oceans will provide a basis for understanding their dominance in particular periods in geological time and determine their possible dominance in the future (fig. S9). This previously unknown finding has profound implications in the dominance of particular groups in the global ocean.

MATERIALS AND METHODS

Data on the number of species belonging to each microalgal group

We analyzed the species belonging to each group of the formally described microalgae and cyanobacteria. These data were obtained from Algaebase (https://www.algaebase.org) in March 2020. Only currently accepted species were included. The categorized microalgal groups were diatoms, dinoflagellates, haptophytes, ochrophytes

including raphidophytes, chlorophytes, cryptophytes, and euglenophytes. However, raphidophytes were separated from ochrophytes because some raphidophyte species caused red tides globally, whereas there were no ochrophytes, except raphidophytes, that caused red tides globally.

Data on the red tides in the world ocean in 1990–2019

We analyzed red tides occurring in the world ocean during 1990–2019 that had been reported in the literature (~800 references; e.g., tables S2 and S3 for the target mixotrophic dinoflagellates). Furthermore, we investigated the causative species of each red tide event and also the country where the red tide event occurred and, lastly, determined the number of the countries in which each red tide species had caused red tides (NoCountry^{RT}).

Data on presence and absence of photosynthesis-related genes in dinoflagellates

To investigate 22 target genes related to photosynthesis (8 photosystem genes, 9 Calvin cycle genes, and 5 gluconeogenesis genes) of major dinoflagellates, the transcriptomes of 3 heterotrophic, 3 kleptoplastidic, 9 mixotrophic, and 2 autotrophic dinoflagellates were analyzed (Fig. 2 and tables S4 to S10). The transcriptomes of the heterotrophic dinoflagellate *Polykrikos kofoidii*, the kleptoplastidic dinoflagellate *G. smaydae*, the mixotrophic dinoflagellates *P. shiwhaense* and *Biecheleria cincta*, and the autotrophic dinoflagellate *Biecheleriopsis adriatica* were newly assembled in this study, but those of the other dinoflagellates were obtained from the literature (table S6). The transcriptome of *Heterocapsa rotundata* was also analyzed to test whether the signal of the presence of photosynthesis-related genes of *G. smaydae* was this predator's own signal or from its prey. On the basis of the assembled transcriptomes, the target genes of the dinoflagellate species were identified using a tBLASTn algorithm as implemented in CLC Genomic Workbench ver. 10.0.1 (QIAGEN N.V. Venlo, the Netherlands) (table S7). Some genes of which phylogenetic relationships need to be confirmed were aligned, and trees were constructed. Furthermore, the presence of *psaA* and *psbB* genes of the dinoflagellates were additionally confirmed on the basis of genomic DNA sequencing (figs. S3 and tables S5 and S8 to S10).

Culturing, sequencing, and sequence assembly of six dinoflagellates

Before the transcriptome experiments were conducted, two consecutive single-cell isolations of cells from each clonal culture of *P. kofoidii* (PKJH1607), *G. smaydae* (GSSH1005), *P. shiwhaense* (PSSH0605), *B. cincta* (BCSW0906), *B. adriatica* (BATY06), and *H. rotundata* (HRSH1201) were performed to confirm no potential contamination by bacteria or other small eukaryotes. Furthermore, to confirm rapid growth condition and no remaining prey cells in each culture, 5 ml of aliquots was taken from each bottle every 2 days and fixed with Lugol's solution (final concentration, 5%). The aliquots were taken from the fixed sample and then transferred to two 1-ml Sedgwick-Rafter chambers for cell enumeration.

For transcriptome analysis, a dense culture (~80 cells ml^{-1}) of *P. kofoidii* growing on *Alexandrium minutum* (CCMP1888) was transferred to an 800-ml culture flask containing dense prey (~6000 cells ml^{-1}) and autoclaved filtered seawater. After prey cells were undetected in the ambient waters (2 days after inoculation), *P. kofoidii* cells were maintained without added prey cells for 3 days (starved for 3 days). For harvesting *P. kofoidii* cells, 800 ml of aliquot containing approximately 168,000 cells was taken from the culture flask and then centrifuged for 5 min at 800*g* using a Vision Centrifuge VS-5500 (Vision Scientific Company, Bucheon, Korea). Similarly, a dense culture (2000 cells ml^{-1}) of *G. smaydae* growing on *H. rotundata* (HRSH1201) was transferred to a 2-liter polycarbonate (PC) bottle containing dense prey (~60,000 cells ml^{-1}). After prey cells were undetectable (3 days after inoculation), *G. smaydae* cells were maintained without added prey cells for 3 days. For harvesting cells, 1.8 liter of aliquot containing approximately 4×10^7 cells was taken from the PC bottle and then centrifuged for 10 min at 1000*g*.

A dense culture (~3000 cells ml^{-1}) of *P. shiwhaense* growing on *Amphidinium carterae* (SIO PY-1) was distributed to an 800-ml culture flask containing dense prey (~5000 cells ml^{-1}). After prey cells were undetectable (2 days after inoculation), *P. shiwhaense* cells were maintained without added prey cells for 18 days. For harvesting cells, 800 ml of aliquot containing approximately 5×10^6 cells was taken from the culture flask and then centrifuged for 10 min at 1000*g*. Moreover, a dense culture (~3000 cells ml^{-1}) of *B. cincta* growing on the raphidophyte *Heterosigma akashiwo* (HAKS9905) was transferred to a 2-liter PC bottle containing dense prey (~25,000 cells ml^{-1}). After a prey cell was undetected in the ambient waters (4 days after inoculation), *B. cincta* cells were maintained without added prey cells for 3 days. For harvesting cells, 1.8 liter of aliquot containing approximately 2×10^7 cells was taken from the PC bottle and then centrifuged for 10 min at 1000*g*.

A dense culture of *B. adriatica* growing autotrophically (~5000 cells ml^{-1}) was distributed to a 2-liter PC bottle containing an autoclaved f/2-Si medium (*25*). For harvesting cells, 500 ml of aliquot containing approximately 5×10^7 cells in its exponential phase (10 days after inoculation) was taken from the PC bottle and then centrifuged for 10 min at 1000*g*. Similarly, a dense culture (~10,000 cells ml^{-1}) of *H. rotundata* growing autotrophically was transferred to an 800-ml culture flask containing an autoclaved f/2-Si medium. Five hundred milliliters of aliquot containing approximately 1×10^7 cells in its exponential phase (7 days after inoculation) was taken from the flask and then centrifuged for 10 min at 1000*g*.

The pellets of the six dinoflagellate samples harvested were immediately frozen with liquid nitrogen and stored at −80°C until RNA extraction. Then, total RNA from each sample was extracted according to the RNeasy Plant Mini Kit protocol (catalog no. 74903; Qiagen, Germany) and treated with the RNase-Free DNase set (catalog no. 79254) to remove any residual genomic DNA. The complementary DNA (cDNA) libraries of *G. smaydae*, *B. cincta*, and *B. adriatica* were sequenced using a HiSeq 2500 system (Illumina Inc., San Diego, CA) by the National Instrumentation Center for Environmental Management (Seoul, Korea). *P. kofoidii*, *P. shiwhaense*, and *H. rotundata* were sequenced using a NovaSeq 6000 system (Illumina Inc., San Diego, CA) by Macrogen (Seoul, Korea). Moreover, the quality of the data used for each assembly was verified using FastQC v.11.6 (*26*). Subsequently, the clean reads of each dinoflagellate species were independently de novo assembled with Trinity software (*27*). The transcriptomes of the six dinoflagellates analyzed in this study were deposited in the National Center for Biotechnology Information (NCBI) Sequence Read Archive (SRA accession numbers SRR11946747, SRR11947552, SRR11994189, SRR11994191, SRR11994206, and SRR12020522).

The data on the transcriptome assembly of the kleptoplastidic dinoflagellate *P. piscicida* and mixotrophic dinoflagellates *Y. yeosuensis* and *Ansanella granifera* were obtained from our previous studies (*28*–*30*). Moreover, the transcriptomic sequences of the heterotrophic dinoflagellates *Oxyrrhis marina*, *Noctiluca scintillans*, kleptoplastidic

dinoflagellate *D. acuminata*, mixotrophic dinoflagellates *Lingulodinium polyedra*, *Gymnodinium catenatum*, *A. andersonii*, *Heterocapsa steinii*, and the autotrophic dinoflagellate *Pelagodinium bei* were obtained from the Marine Microbial Eukaryote Transcriptome Sequencing Project (table S6) (*31*, *32*).

Gene identification

The presence or absence and transcript sequences of target genes encoding for plastid-related proteins in these dinoflagellates was identified using a tBLASTn algorithm as implemented in CLC Genomic Workbench ver. 10.0.1 (QIAGEN N.V. Venlo, the Netherlands). We used a stringent *E*-value cutoff criterion of *E*-20. The amino acid sequences of the previously well-identified plastid genes were used as queries to perform tBLASTn searches (table S7). Among the plastid genes belonging to photosystem I and photosystem II, only the genes commonly identified on minicircles of dinoflagellates were analyzed in this study (Fig. 2 and table S4) (*33*, *34*). Regarding query sequences of the *psbI* gene, however, identifying its orthologous genes of dinoflagellates was impossible due to its small sequence size (approximately 35 to 38 amino acids). Moreover, the possible presence of prey-originated plastid gene sequences in the transcriptome of *G. smaydae* was further confirmed using the strict criteria of the BLASTn algorithm (cutoff *E*-value <*E*-100 and identity >99%) against the transcriptome of the prey *H. rotundata*. Similarly, the identified plastid genes of the other dinoflagellates grown heterotrophically or kleptoplastically also needed to be analyzed to determine whether they are potentially evolutionarily remnant genes or just remained genes from the prey materials. However, there have been no data about the clonal strain of the prey transcriptomes, except for *G. smaydae*, and thus, we carried out additional homology searches for these genes against the NCBI nonredundant database. If the homology of the gene was highly similar (i.e., cutoff *E*-value <*E*-100 and identity >95%) to that of any species in the genus to which the prey species belongs, then we considered this gene as a prey-originated gene and did not include it in the heatmap. Moreover, these relationships were further validated on the basis of phylogenetic analysis (see the next section).

Phylogenetic analysis for gene validation

Some genes that were present in some dinoflagellates but absent in others were aligned with multiple sequences by MEGA v.4 (*35*). The alignments of the tBLASTn hits were manually inspected and curated to remove problematic sequences (i.e., chimeric sequences and/or contaminant sequences), and the ambiguously aligned sites were further removed. In this study, the nucleotide sequence–based phylogenies were constructed to eliminate the possibility that fragmented sequences of potential genes are filtered through the decoding process. The phylogenetic analyses were performed under the GTR+G model and inferred by Bayesian analysis using the MrBayes v.3.1 program (*36*). Bayesian analysis was sampled every 200 generations and continued until the average SD of the split frequencies dropped below 0.01. Moreover, it was confirmed that the analyses reached statistical stationarity well before the burn-in period by plotting the ln-likelihood of the sampled trees against generation time.

Genomic DNA sequencing for gene validation

Since the coding region of plastid genes that we analyzed in this study consisted of a single exon without internal introns, we confirmed the presence of a few identified transcripts (i.e., cDNA of *psaA* and *psbB*) by genomic DNA sequencing. Especially, since all the genes in the photosystem identified from the transcriptome of *G. smaydae* were identical to those of its prey *H. rotundata* (i.e., no possession of its own genes), we confirmed whether these genes existed inside *G. smaydae* cells until the cells were almost dead (after 10-day starvation). Thus, we designed the universal polymerase chain reaction (PCR) primers for partial sequences of *psaA* and *psbB* genes of the dinoflagellate species listed in tables S8 to S10. To determine the universal sequences, manual searches of the alignments were conducted using the program MEGA v.4. The sequences for the forward and reverse primers for *psaA* and *psbB* genes were selected from the regions that are conserved from all the aligned dinoflagellate species (table S10). The primer sequences were analyzed with Primer 3 (Whitehead Institute and Howard Hughes Medical Institute, MD) and Oligo Calc: Oligonucleotide Properties Calculator (*37*) for optimal melting temperature and secondary structure.

For PCR amplification, the genomic DNAs of some target dinoflagellate species (i.e., 2-day starved *G. smaydae*, 10-day starved *G. smaydae*, 5-day starved *Y. yeosuensis*, and autotrophically growing *A. carterae*, *H. rotundata*, and *G. catenatum*) were extracted using the AccuPrep Genomic DNA Extraction Kit (Bioneer, Daejeon, Korea), according to the manufacturer's instructions. The PCR conditions were as follows: initial denaturation at 95°C for 2 min; followed by 35 cycles at 95°C for 20 s, an appropriate annealing temperature for 40 s, and 72°C for 1 min, with a final elongation step at 72°C for 5 min. The annealing temperature was adjusted for specific primer sets according to the manufacturer's instructions. The detailed methods for PCR amplification, sequencing, and alignment were according to the procedures used by Jang *et al.* (*38*). If the PCR product mixed with 0.5 μl of goRed fluorescent reagent (Genepole, Seoul, Korea) was not identified from the first amplification as checked using gel electrophoresis, then the second DNA amplification using the same primer sets was performed with the 1 μl of the first PCR product as a template. As a result, the presence or absence of *psaA* and *psbB* genes identified from transcriptomic data could be verified by sequencing genomic DNA of partial 400 to 500 lengths of *psaA* and *psbB* genes (table S5).

Data acquisition for the calculation of two mixotrophic ability indices

We developed two new indices of mixotrophic ability of a mixotrophic dinoflagellate—predation contribution to total growth rate ($PredC^{TGR}$) and the ratio of the number of edible prey taxa to that of total tested prey taxa (RET^{PREY}). We selected mixotrophic dinoflagellates of which both autotrophic (without added prey, GR^{Auto}) and total or mixotrophic growth rates (with added prey, GR^{Total}) had been reported (table S11).

The $PredC^{TGR}$ of a mixotrophic dinoflagellate under a given prey concentration, temperature, and light condition was calculated as follows

$$PredC^{TGR}(\%) = (GR^{Total} - GR^{Auto}) / GR^{Total} \times 100$$

We did not calculate $PredC^{TGR}$ when both GR^{Total} and GR^{Auto} were negative. Furthermore, we gave the $PredC^{TGR}$ value of 100% when GR^{Auto} was zero or negative, whereas GR^{Total} was positive. In a rare case, GR^{Auto} was slightly greater than GR^{Total}. We gave the $PredC^{TGR}$ value of 0% in this case.

We calculated the ratio of the number of edible prey taxa to that of total tested prey taxa (RET^{PREY}) of a mixotrophic dinoflagellate rather than the absolute number of edible prey because the prey species for one mixotrophic dinoflagellate species were sometimes different from those of the other mixotrophic dinoflagellate species

in different literature. In this calculation, we included the mixotrophic dinoflagellate species for which the number of total tested prey taxa was ≥5 species. Engulfment-feeding mixotrophic dinoflagellates usually do not feed on prey larger than themselves, and thus, we excluded the prey species larger than themselves from the nominator (i.e., total tested prey taxa) when the target mixotrophic dinoflagellates were engulfment feeders.

Statistical analysis

The simple linear regression was used to examine relationships between variables (i.e., $PredC^{TGR}$, RET^{PREY}, $NoCountry^{RT}$, GR^{Max}, and equivalent spherical diameter). All analyses were performed using SPSS ver. 25.0 (IBM-SPSS Inc., Armonk, NY). A 0.05 significance criterion was chosen.

SUPPLEMENTARY MATERIALS

Supplementary material for this article is available at http://advances.sciencemag.org/cgi/content/full/7/2/eabe4214/DC1

View/request a protocol for this paper from *Bio-protocol*.

REFERENCES AND NOTES

1. P. G. Falkowski, R. T. Barber, V. Smetacek, Biogeochemical controls and feedbacks on ocean primary production. *Science* **281**, 200–206 (1998).
2. M. J. Behrenfeld, R. T. O'Malley, D. A. Siegel, C. R. McClain, J. L. Sarmiento, G. C. Feldman, A. J. Milligan, P. G. Falkowski, R. M. Letelier, E. S. Boss, Climate-driven trends in contemporary ocean productivity. *Nature* **444**, 752–755 (2006).
3. H. J. Jeong, Y. D. Yoo, J. S. Kim, K. A. Seong, N. S. Kang, T. H. Kim, Growth, feeding and ecological roles of the mixotrophic and heterotrophic dinoflagellates in marine planktonic food webs. *Ocean Sci. J.* **45**, 65–91 (2010).
4. A. Z. Worden, M. J. Follows, S. J. Giovannoni, S. Wilken, A. E. Zimmerman, P. J. Keeling, Rethinking the marine carbon cycle: Factoring in the multifarious lifestyles of microbes. *Science* **347**, 1257594 (2015).
5. P. G. Falkowski, M. E. Katz, A. H. Knoll, A. Quigg, J. A. Raven, O. Schofield, F. J. R. Taylor, The evolution of modern eukaryotic phytoplankton. *Science* **305**, 354–360 (2004).
6. X. Irigoien, J. Huisman, R. P. Harris, Global biodiversity patterns of marine phytoplankton and zooplankton. *Nature* **429**, 863–867 (2004).
7. M. E. Katz, Z. V. Finkel, D. Grzebyk, A. H. Knoll, P. G. Falkowski, Evolutionary trajectories and biogeochemical impacts of marine eukaryotic phytoplankton. *Annu. Rev. Ecol. Evol. Syst.* **35**, 523–556 (2004).
8. A.-S. Benoiston, F. M. Ibarbalz, L. Bittner, L. Guidi, O. Jahn, S. Dutkiewicz, C. Bowler, The evolution of diatoms and their biogeochemical functions. *Philosoph. Trans. R. Soc. B Biol. Sci.* **372**, 20160397 (2017).
9. H. J. Jeong, Y. D. Yoo, K. H. Lee, T. H. Kim, K. A. Seong, N. S. Kang, S. Y. Lee, J. S. Kim, S. Kim, W. H. Yih, Red tides in Masan Bay, Korea in 2004–2005: I. Daily variations in the abundance of red-tide organisms and environmental factors. *Harmful Algae* **30**, S75–S88 (2013).
10. D. M. Anderson, Turning back the harmful red tide. *Nature* **388**, 513–514 (1997).
11. C. A. Heil, P. M. Glibert, C. Fan, *Prorocentrum minimum* (Pavillard) Schiller: A review of a harmful algal bloom species of growing worldwide importance. *Harmful Algae* **4**, 449–470 (2005).
12. I. Cahyanto, B. Liu-Lastres, Risk perception, media exposure, and visitor's behavior responses to Florida Red Tide. *J. Trav. Tour. Mark.* **37**, 447–459 (2020).
13. A. Mitra, K. J. Flynn, U. Tillmann, J. A. Raven, D. Caron, D. K. Stoecker, F. Not, P. J. Hansen, G. Hallegraeff, R. Sanders, S. Wilken, G. McManus, M. Johnson, P. Pitta, S. Våge, T. Berge, A. Calbet, F. Thingstad, H. J. Jeong, J. Burkholder, P. M. Glibert, E. Granéli, V. Lundgren, Defining planktonic protist functional groups on mechanisms for energy and nutrient acquisition: Incorporation of diverse mixotrophic strategies. *Protist* **167**, 106–120 (2016).
14. K. J. Flynn, A. Mitra, K. Anestis, A. A. Anschütz, A. Calbet, G. D. Ferreira, N. Gypens, P. J. Hansen, U. John, J. L. Martin, J. S. Mansour, M. Maselli, N. Medić, A. Norlin, F. Not, P. Pitta, F. Romano, E. Saiz, L. K. Schneider, W. Stolte, C. Traboni, Mixotrophic protists and a new paradigm for marine ecology: Where does plankton research go now? *J. Plankton Res.* **41**, 375–391 (2019).
15. D. K. Stoecker, P. J. Hansen, D. A. Caron, A. Mitra, Mixotrophy in the marine plankton. *Ann. Rev. Mar. Sci.* **9**, 311–335 (2017).
16. M. G. Park, S. Kim, H. S. Kim, G. Myung, Y. G. Kang, W. Yih, First successful culture of the marine dinoflagellate *Dinophysis acuminata*. *Aquat. Microbial Ecol.* **45**, 101–106 (2006).
17. H. J. Jeong, Y. D. Yoo, N. S. Kang, A. S. Lim, K. A. Seong, S. Y. Lee, M. J. Lee, K. H. Lee, H. S. Kim, W. Shin, S. W. Nam, W. Yih, K. Lee, Heterotrophic feeding as a newly identified survival strategy of the dinoflagellate *Symbiodinium*. *Proc. Nat. Acad. Sci. U.S.A.* **109**, 12604–12609 (2012).
18. D. A. Caron, Mixotrophy stirs up our understanding of marine food webs. *Proc. Natl. Acad. Sci. U.S.A.* **113**, 2806–2808 (2016).
19. E. Hehenberger, R. J. Gast, P. J. Keeling, A kleptoplastidic dinoflagellate and the tipping point between transient and fully integrated plastid endosymbiosis. *Proc. Natl. Acad. Sci. U.S.A.* **116**, 17934–17942 (2019).
20. S. B. Yamada, E. G. Boulding, Claw morphology, prey size selection and foraging efficiency in generalist and specialist shell-breaking crabs. *J. Exp. Mar. Biol. Ecol.* **220**, 191–211 (1998).
21. J. Terraube, D. Guixé, B. Arroyo, Diet composition and foraging success in generalist predators: Are specialist individuals better foragers? *Basic Appl. Ecol.* **15**, 616–624 (2014).
22. L. F. García, C. Viera, S. Pekár, Comparison of the capture efficiency, prey processing, and nutrient extraction in a generalist and a specialist spider predator. *Sci. Nat.* **105**, 30 (2018).
23. S. H. Jang, H. J. Jeong, Spatio-temporal distributions of the newly described mixotrophic dinoflagellate *Yihiella yeosuensis* (Suessiaceae) in Korean coastal waters and its grazing impact on prey populations. *Algae* **35**, 45–59 (2020).
24. S. Y. Lee, H. J. Jeong, J. H. Ok, H. C. Kang, J. H. You, Spatial-temporal distributions of the newly described mixotrophic dinoflagellate *Gymnodinium smaydae* in Korean coastal waters. *Algae* **35**, 225–236 (2020).
25. R. R. Guillard, J. H. Ryther, Studies of marine planktonic diatoms: I. *Cyclotella nana* Hustedt, and *Detonula confervacea* (Cleve) Gran. *Can. J. Microbiol.* **8**, 229–239 (1962).
26. S. Andrews, FastQC: A quality control tool for high throughput sequence data (2010); http://www.bioinformatics.babraham.ac.uk/projects/fastqc [accessed May 2017-Dec 2019].
27. B. J. Haas, A. Papanicolaou, M. Yassour, M. Grabherr, P. D. Blood, J. Bowden, M. B. Couger, D. Eccles, B. Li, M. Lieber, M. D. MacManes, M. Ott, J. Orvis, N. Pochet, F. Strozzi, N. Weeks, R. Westerman, T. William, C. N. Dewey, R. Henschel, R. D. LeDuc, N. Friedman, A. Regev, De novo transcript sequence reconstruction from RNA-seq using the Trinity platform for reference generation and analysis. *Nat. Protocol.* **8**, 1494–1512 (2013).
28. G. H. Kim, H. J. Jeong, Y. D. Yoo, S. Kim, J. H. Han, J. W. Han, G. C. Zuccarello, Still acting green: Continued expression of photosynthetic genes in the heterotrophic dinoflagellate *Pfiesteria piscicida* (Peridiniales, Alveolata). *PLOS ONE* **8**, e68232 (2013).
29. S. H. Jang, H. J. Jeong, J. K. Chon, S. Y. Lee, De novo assembly and characterization of the transcriptome of the newly described dinoflagellate *Ansanella granifera*: Spotlight on flagellum-associated genes. *Mar. Genom.* **33**, 47–55 (2017).
30. S. H. Jang, H. J. Jeong, J. K. Chon, De novo transcriptome of the newly described phototrophic dinoflagellate *Yihiella yeosuensis*: Comparison between vegetative cells and cysts. *Mar. Biol.* **166**, 104 (2019).
31. P. J. Keeling, F. Burki, H. M. Wilcox, B. Allam, E. E. Allen, L. A. Amaral-Zettler, E. V. Armbrust, J. M. Archibald, A. K. Bharti, C. J. Bell, B. Beszteri, K. D. Bidle, C. T. Cameron, L. Campbell, D. A. Caron, R. A. Cattolico, J. L. Collier, K. Coyne, S. K. Davy, P. Deschamps, S. T. Dyhrman, B. Edvardsen, R. D. Gates, C. J. Gobler, S. J. Greenwood, S. M. Guida, J. L. Jacobi, K. S. Jakobsen, E. R. James, B. Jenkins, U. John, M. D. Johnson, A. R. Juhl, A. Kamp, L. A. Katz, R. Kiene, A. Kudryavtsev, B. S. Leander, S. Lin, C. Lovejoy, D. Lynn, A. Marchetti, G. McManus, A. M. Nedelcu, S. Menden-Deuer, C. Miceli, T. Mock, M. Montresor, M. A. Moran, S. Murray, G. Nadathur, S. Nagai, P. B. Ngam, B. Palenik, J. Pawlowski, G. Petroni, G. Piganeau, M. C. Posewitz, K. Rengefors, G. Romano, M. E. Rumpho, T. Rynearson, K. B. Schilling, D. C. Schroeder, A. G. B. Simpson, C. H. Slamovits, D. R. Smith, G. J. Smith, S. R. Smith, H. M. Sosik, P. Stief, E. Theriot, S. N. Twary, P. E. Umale, D. Vaulot, B. Wawrik, G. L. Wheeler, W. H. Wilson, Y. Xu, A. Zingone, A. Z. Worden, The Marine Microbial Eukaryote Transcriptome Sequencing Project (MMETSP): Illuminating the functional diversity of eukaryotic life in the oceans through transcriptome sequencing. *PLOS Biol.* **12**, e1001889 (2014).
32. L. K. Johnson, H. Alexander, C. T. Brown, Re-assembly, quality evaluation, and annotation of 678 microbial eukaryotic reference transcriptomes. *GigaScience* **8**, giy158 (2019).
33. A. C. Barbrook, N. Santucci, L. J. Plenderleith, R. G. Hiller, C. J. Howe, Comparative analysis of dinoflagellate chloroplast genomes reveals rRNA and tRNA genes. *BMC Genomics* **7**, 297 (2006).
34. C. J. Howe, R. E. R. Nisbet, A. C. Barbrook, The remarkable chloroplast genome of dinoflagellates. *J. Exp. Bot.* **59**, 1035–1045 (2008).
35. K. Tamura, J. Dudley, M. Nei, S. Kumar, MEGA4: Molecular evolutionary genetics analysis (MEGA) software version 4.0. *Mol. Boil. Evol.* **24**, 1596–1599 (2007).
36. J. P. Huelsenbeck, F. Ronquist, MRBAYES: Bayesian inference of phylogenetic trees. *Bioinformatics* **17**, 754–755 (2001).
37. W. A. Kibbe, OligoCalc: An online oligonucleotide properties calculator. *Nucl. Acids Res.* **35**, W43–W46 (2007).
38. S. H. Jang, H. J. Jeong, Y. D. Yoo, *Gambierdiscus jejuensis* sp. nov., an epiphytic dinoflagellate from the waters of Jeju Island, Korea, effect of temperature on the growth, and its global distribution. *Harmful Algae* **80**, 149–157 (2018).

39. P. J. Hansen, K. Ojamäe, T. Berge, E. C. Trampe, L. T. Nielsen, I. Lips, M. Kühl, Photoregulation in a kleptochloroplastidic dinoflagellate, *Dinophysis acuta*. *Frontiers Microbiol.* **7**, 785 (2016).
40. K. H. Lee, H. J. Jeong, T. Y. Jang, A. S. Lim, N. S. Kang, J. H. Kim, K. Y. Kim, K. T. Park, K. Lee, Feeding by the newly described mixotrophic dinoflagellate *Gymnodinium smaydae*: Feeding mechanism, prey species, and effect of prey concentration. *J. Exp. Mar. Biol. Ecol.* **459**, 114–125 (2014a).
41. H. do Rosário Gomes, J. I. Goes, S. P. Matondkar, E. J. Buskey, S. Basu, S. Parab, P. Thoppil, Massive outbreaks of *Noctiluca scintillans* blooms in the Arabian Sea due to spread of hypoxia. *Nat. Commun.* **5**, 4862 (2014).
42. P. J. Hansen, L. Miranda, L. R. Azanza, Green *Noctiluca scintillans*: A dinoflagellate with its own greenhouse. *Mar. Ecol. Prog. Ser.* **275**, 79–87 (2004).
43. A. H. Knoll, M. J. Follows, A bottom-up perspective on ecosystem change in Mesozoic oceans. *Proc. R. Soc. B Biol. Sci.* **283**, 20161755 (2016).
44. J. Janouškovec, G. S. Gavelis, F. Burki, D. Dinh, T. R. Bachvaroff, S. G. Gornik, K. J. Bright, B. Imanian, S. L. Strom, C. F. Delwiche, R. F. Waller, R. A. Fensome, B. S. Leander, F. L. Rohwer, J. F. Saldarriaga, Major transitions in dinoflagellate evolution unveiled by phylotranscriptomics. *Proc. Natl. Acad. Sci. U.S.A.* **114**, E171–E180 (2017).
45. S. H. Jang, H. J. Jeong, J. E. Kwon, K. H. Lee, Mixotrophy in the newly described dinoflagellate *Yihiella yeosuensis*: A small, fast dinoflagellate predator that grows mixotrophically, but not autotrophically. *Harmful Algae* **62**, 94–103 (2017).
46. S. K. Lee, H. J. Jeong, S. H. Jang, K. H. Lee, N. S. Kang, M. J. Lee, É. Potvin, Mixotrophy in the newly described dinoflagellate *Ansanella granifera*: Feeding mechanism, prey species, and effect of prey concentration. *Algae* **29**, 137–152 (2014).
47. T. C. LaJeunesse, J. E. Parkinson, P. W. Gabrielson, H. J. Jeong, J. D. Reimer, C. R. Voolstra, S. R. Santos, Systematic revision of Symbiodiniaceae highlights the antiquity and diversity of coral endosymbionts. *Curr. Biol.* **28**, 2570–2580.e6 (2018).
48. K. Koike, H. Sekiguchi, A. Kobiyama, K. Takishita, M. Kawachi, K. Koike, T. Ogata, A novel type of kleptoplastidy in *Dinophysis* (Dinophyceae): Presence of haptophyte-type plastid in *Dinophysis mitra*. *Protist* **156**, 225–237 (2005).
49. J. H. Wisecaver, J. D. Hackett, Transcriptome analysis reveals nuclear-encoded proteins for the maintenance of temporary plastids in the dinoflagellate *Dinophysis acuminata*. *BMC Genomics* **11**, 366 (2010).
50. J. H. You, H. J. Jeong, A. S. Lim, J. H. Ok, H. C. Kang, Effects of irradiance and temperature on the growth and feeding of the obligate mixotrophic dinoflagellate *Gymnodinium smaydae*. *Mar. Biol.* **167**, 64 (2020).
51. Y. D. Yoo, H. J. Jeong, N. S. Kang, J. Y. Song, K. Y. Kim, G. Lee, J. Kim, Feeding by the newly described mixotrophic dinoflagellate *Paragymnodinium shiwhaense*: Feeding mechanism, prey species, and effect of prey concentration. *J. Eukaryot. Microbiol.* **57**, 145–158 (2010).
52. H. J. Jeong, K. H. Lee, Y. D. Yoo, N. S. Kang, J. Y. Song, T. H. Kim, K. A. Seng, J. S. Kim, É. Potvin, Effects of light intensity, temperature, and salinity on the growth and ingestion rates of the red-tide mixotrophic dinoflagellate *Paragymnodinium shiwhaense*. *Harmful Algae* **80**, 46–54 (2018).
53. N. S. Kang, H. J. Jeong, Y. D. Yoo, E. Y. Yoon, K. H. Lee, K. Lee, G. Kim, Mixotrophy in the newly described phototrophic dinoflagellate *Woloszynskia cincta* from western Korean waters: Feeding mechanism, prey species and effect of prey concentration. *J. Eukaryot. Microbiol.* **58**, 152–170 (2011).
54. J. H. Ok, H. J. Jeong, A. S. Lim, J. H. You, H. C. Kang, S. J. Kim, S. Y. Lee, Effects of light and temperature on the growth of *Takayama helix* (Dinophyceae): Mixotrophy as a survival strategy against photoinhibition. *J. Phycol.* **55**, 1181–1195 (2019).
55. A. S. Lim, H. J. Jeong, J. H. Kim, S. H. Jang, M. J. Lee, K. Lee, Mixotrophy in the newly described dinoflagellate *Alexandrium pohangense*: A specialist for feeding on the fast-swimming ichthyotoxic dinoflagellate *Cochlodinium polykrikoides*. *Harmful Algae* **49**, 10–18 (2015).
56. A. S. Lim, H. J. Jeong, J. H. Ok, J. H. You, H. C. Kang, S. J. Kim, Effects of light intensity and temperature on growth and ingestion rates of the mixotrophic dinoflagellate *Alexandrium pohangense*. *Mar. Biol.* **166**, 98 (2019).
57. H. J. Jeong, J. H. Ok, A. S. Lim, J. E. Kwon, S. J. Kim, S. Y. Lee, Mixotrophy in the phototrophic dinoflagellate *Takayama helix* (family Kareniaceae): Predator of diverse toxic and harmful dinoflagellates. *Harmful Algae* **60**, 92–106 (2016).
58. H. J. Jeong, Y. D. Yoo, J. S. Kim, T. H. Kim, J. H. Kim, N. S. Kang, W. Yih, Mixotrophy in the phototrophic harmful alga *Cochlodinium polykrikoides* (Dinophycean): Prey species, the effects of prey concentration, and grazing impact. *J. Eukaryot. Microbiol.* **51**, 563–569 (2004).
59. H. J. Jeong, Y. D. Yoo, J. Y. Park, J. Y. Song, S. T. Kim, S. H. Lee, K. Y. Kim, W. Yih, Feeding by phototrophic red-tide dinoflagellates: Five species newly revealed and six species previously known to be mixotrophic. *Aquat. Microb. Ecol.* **40**, 133–150 (2005).
60. H. J. Jeong, Y. D. Yoo, N. S. Kang, J. R. Rho, K. A. Seong, J. W. Park, G. S. Nam, W. Yih, Ecology of *Gymnodinium aureolum*. I. Feeding in western Korean waters. *Aquat. Microb. Ecol.* **59**, 239–255 (2010).
61. K. H. Lee, H. J. Jeong, J. E. Kwon, H. C. Kang, J. H. Kim, S. H. Jang, J. Y. Park, E. Y. Yoon, J. S. Kim, Mixotrophic ability of the phototrophic dinoflagellates *Alexandrium andersonii*, *A. affine*, and *A. fraterculus*. *Harmful Algae* **59**, 67–81 (2016).
62. H. J. Jeong, Y. D. Yoo, K. A. Seong, J. H. Kim, J. Y. Park, S. Kim, S. H. Lee, J. H. Ha, W. H. Yih, Feeding by the mixotrophic red-tide dinoflagellate *Gonyaulax polygramma*: Mechanisms, prey species, effects of prey concentration, and grazing impact. *Aquat. Microb. Ecol.* **38**, 249–257 (2005).
63. A. S. Lim, H. J. Jeong, J. H. Ok, S. J. Kim, Feeding by the harmful phototrophic dinoflagellate *Takayama tasmanica* (Family Kareniaceae). *Harmful Algae* **74**, 19–29 (2018).

Acknowledgments: We thank N. S. Kang, J. S. Kim, and K. A. Seong for technical support. **Funding:** H.J.J. was funded by the Useful Dinoflagellate program of the Korea Institute of Marine Science and Technology Promotion and the National Research Foundation (NRF-2017R1E1A1A01074419 and NRF-2020M3F6A1110582). **Author contributions:** H.J.J., H.C.K., and S.H.J. designed the study. H.J.J., H.C.K., A.S.L., S.H.J., S.Y.L., J.H.O., J.H.Y., J.H.K., K.H.L., S.A.P., S.H.E., and Y.D.Y. obtained the data and conducted the experiments. H.J.J., H.C.K., A.S.L., and S.H.J. performed the analyses. H.J.J., H.C.K., K.L., and K.Y.K. drafted the manuscript. All authors discussed the results. **Competing interests:** The authors declare that they have no competing interests. **Data and materials availability:** All data needed to evaluate the conclusions in the paper are present in the paper and/or the Supplementary Materials. Additional data related to this paper may be requested from the authors.

Submitted 20 August 2020
Accepted 16 November 2020
Published 8 January 2021
10.1126/sciadv.abe4214

Citation: H. J. Jeong, H. C. Kang, A. S. Lim, S. H. Jang, K. Lee, S. Y. Lee, J. H. Ok, J. H. You, J. H. Kim, K. H. Lee, S. A. Park, S. H. Eom, Y. D. Yoo, K. Y. Kim, Feeding diverse prey as an excellent strategy of mixotrophic dinoflagellates for global dominance. *Sci. Adv.* **7**, eabe4214 (2021).